Joint Communication and Control for mmWave/THz Beam Alignment in V2X Networks

Bo Chang, Xiaoyu Yan, Lei Zhang, Zhi Chen, Lingxiang Li, and Muhammad Ali Imran

***Abstract*—As promising candidate frequency bands, millimeter wave (mmWave) and terahertz (THz) communications can provide ultra-high transmission rate to enable vehicle-to-everything (V2X) networks for connected autonomous vehicles (CAV). However, beam alignment is extremely challenging in mmWave/THz communications due to its narrow beam-width and fast mobility of CAV. In this paper, we propose a new joint communication and control algorithm for beam alignment, where the mutual positive effect of communications and motion control of CAV on each other is discussed. Specifically, we first provide a framework to show the interaction between motion control of CAV and beam alignment of transmission from base station (BS) to CAV. Then, we analyze the effect of CAV control on beam alignment in communications, where a theorem is obtained to show the closed-form expression of their relationship. Finally, we discuss the CAV control design affected by beam alignment. Simulation results show remarkable performance of the proposed method.**

***Index Terms*—V2X, CAV, mmWave and THz communications, beam alignment, joint communication and control.**

I. Introduction

DRIVEN by the advances in 5G, artificial intelligence (AI), sensing techniques, cloud/edge computing, etc., vehicle-to-everything (V2X) networks are enabling a transition from connected vehicles (CV) to connected autonomous vehicles (CAV) [1]–[3], which are connected to each other or infrastructure for exchanging road or safety related information. With the assistance of sensed information by massively deployed sensors (e.g., Lidar or Radar) embedded in vehicles or along the road, high autonomous driving level, e.g., L4 or L5 autonomous driving of CAV, can be achieved with little or no human control in the near future. Furthermore, a huge amount of data are needed to be transmitted to CAV to guarantee the entertainment of the passengers. As a result, there can be 4 TB data generated for CAV every hour [4] [5]. Unfortunately, today's wireless networks are lagging far behind in their ability to support ultra-high data rate [6] [7]. For instance, it has been reported that the capacity of the frequency band less than 60 GHz can hardly provide transmission rate more than Gigabits per second (Gbps) [8] [9].

B. Chang, X. Yan, Z. Chen, and L. Li are with the National Key Lab. on Communications, University of Electronic Science and Technology of China (UESTC), Chengdu, 611731, China (e-mail: changb3212@163.com; yanxiaoyu@std.uestc.edu.cn; chenzhi@uestc.edu.cn; lingxiang.li@uestc.edu.cn).

L. Zhang and M. A. Imran are with the School of Engineering, University of Glasgow, Glasgow, G12 8QQ, UK (e-mail: Lei.Zhang@glasgow.ac.uk; muhammad.imran@glasgow.ac.uk).

As promising candidate frequency bands, high frequency millimeter wave (mmWave) and terahertz (THz) communications have the potential to meet the aforementioned data requirement by providing ultra-high transmission rate, i.e., tens of Gbps or even several Terabits per second (Tbps) [9]–[11]. There are two benefits can be provided in mmWave/THz communication enabled V2X networks for CAV. First, as the aforementioned discussion, the ultra-high data rate required in safe driving and entertainment of CAV can be fully guaranteed. Second, through trading time resource by frequency resource, the transmission latency can be significantly reduced by the ultra-wide band (UWB), which means that ultra-reliable and low-latency communication (URLLC) can be provided by high frequency bands to enable cellular assisted real-time motion control of CAV, thus enhancing safe driving [12]. In the following this paper, we adopt mmWave frequency band as an example to develop the proposed method, which can be extended into THz band straightforwardly.

However, it is extremely challenging to adopt mmWave communications since the alignment of narrow beam-width in mmWave is very difficult for high-speed CAV [13]–[16]. Conventional beam alignment methods have difficulties of dealing with the above issue efficiently because of the high complexity or heavy resource consumption [17]–[21]. For instance, according to [18], a bidirectional transmission between transceiver is required to obtain essential information (e.g, vehicle's position) for conventional beam alignment in the 3rd generation partnerships project (3GPP), which results in heavy signal overhead since high mobility of CAV requires frequent beam tracking. For example, for a Cassegrain antenna working at 220 GHz, the effective beamwidth is about 0.3° [9]. If a vehicle is moving with velocity about 120 km/h and about 100 m distance from the transmission antenna, the effective beamwidth is about 10 m, which can be only covered in tens of millisecond (ms) with such high velocity. Then, the essential information for motion control should be received in tens of ms level. Otherwise, the vehicle would be out of the effective beamwidth. It is extremely difficult to deal with such high frequent beam tracking, and meanwhile provide sufficient time resource for data transmission in wireless communications. On the other hand, beam-sweeping is another important beam alignment method [22]–[26]. For instance, in [25], the proposed method first finds the receiver with low accuracy by wide beam, and then obtain the position of the receiver with high accuracy using narrow beam. Furthermore, joint communication and radar based beam alignment method attracts a lot of interest from researchers, where the base station (BS) works as a radar to locate the receiver for beam

alignment [27]. This method can be treated as localization-based alignment method, which works well in relatively static environment. However, when the vehicle is moving with high speed, e.g., the maximum speed in motorway is about 120 km/h, the resource consumption would be very high in frequent scanning with tens of ms level in the aforementioned scanning method and joint communication and radar method. In addition, since too much time resource is spent on scanning and localization, the issue that little time resource for data transmission also exists.

In fact, massive distributed sensors embedded in vehicles or deployed along the road can provide high precision vehicle's information and environmental information (e.g. traffic information on the road) for automatic driving. Such high precision information provides a potential solution for beam alignment in mmWave communications. If a controller embedded in BS can obtain the above high precision information from sensors, the controller can provide its own control command to enhance automatic driving, which is cellular assisted motion control [28]. The overall control loop of cellular assisted motion control begins from sampling at the sensor. Then, the controller at BS receives the sampled information and calculates control command. Finally, CAV receives the control command and update the vehicle's position, velocity, etc. Then, the beam alignment can be operated by the sampled high precision information of CAV during cellular assisted motion control. On the other hand, if the beam is misalignment, the channel capacity would be reduced significantly. Then, the control information in cellular assisted real-time motion control can be discarded since the channel capacity cannot guarantee quality-of-service (QoS) in URLLC. As a result, the cellular assisted real-time motion control would be failed. In addition, the required data rate cannot be maintained when the beam is misalignment.

The heavy resource consumption in conventional beam alignment methods can be solved in the aforementioned beam alignment during cellular assisted motion control. However, high frequent control information update from the sensor to BS is introduced. If the cellular assisted control loop is operated by constant periodical time triggered control, the control loop would be updated with the same high frequency as that from sensor to BS. Then, a lot of resource would be consumed in the control loop. In addition, the issue that little time resource for data transmission from BS to CAV is still not solved.

To lower control information update frequency, provide more time resource for data transmission from BS to CAV, and further reduce resource consumption in cellular assisted motion control, a new event-triggered control policy is considered in this paper. Such event control policies are promising in motion control [29]. Only when some triggering event occurs, the control loop for state update would be activated. However, the control loop is usually activated by some control events, e.g., the difference between the estimated state and actual state exceeding a certain threshold, which is usually from control perspective. Based on that, the communication resource allocation is conducted [29]. On the contrary, this paper considers a new activation criterion from communication perspective. When the data rate requirement cannot be guaranteed because of the beam misalignment, the cellular assisted motion control loop would be activated to update the state of CAV (e.g., vehicle's position, velocity, and direction), and meanwhile the information of CAV at BS would be updated. When the cellular assisted motion control is not activated, the controller embedded in BS would not receive the sensed information. In this case, there would be no control command transmitted from BS to CAV. Then, more time resource for data transmission from BS to CAV can be provided. Compared with constant periodical time triggered control, communication resource consumption can be further reduced in the proposed event-triggered control policy.

However, when the transmission is not activated, the event-triggered control policy would enlarge the state error between the real state of CAV and that known at BS. Since the accuracy of the beam alignment is directly determined by the state error, the misalignment would increase when the motion control is not activated. It leads to that the required data rate cannot be guaranteed in this case. Thus, both the event-triggered cellular assisted control design and required data rate of CAV should be jointly taken into consideration in beam alignment design at the BS, which is joint communication and control for beam alignment design. We notice that some works were done on motion control based beam alignment [28]. However, the interaction between communication and control is lacked in these works. In addition, the motion control prediction of autonomous vehicles in [28] is based on ideal scenario, where the movement of the vehicles is predicted by GPS with a preplanned path or a constrained path, instead of the kinematic model of CAV. This assumption is too strong to be used in real scenarios. For instance, in urban road, the road condition and surrounding environment are very complex. Then, the information of the vehicles (e.g., velocity, direction, and position) may change rapidly, which would result in significant error of the GPS-based prediction method. Therefore, the beam misalignment would be enlarged. Furthermore, the effect of the data rate loss caused by beam misalignment on the control prediction design is missed in [28]. Then, the system design jointly considering the positive interaction between beam alignment from communication perspective and motion control from control perspective cannot be operated.

In this paper, we propose a new joint communication and control algorithm for beam alignment to deal with the above issues. In the proposed method, we first discuss how to utilize the sensed information in both transmission scheduling of the event-triggered cellular assisted motion control and beam alignment in mmWave communications. Then, we analyze how to guarantee data requirement by beam alignment in mmWave communications, which is conducted by the event-triggered motion control design. Here, the data requirement is treated as a threshold in the event-triggered motion control design. In summary, the main contributions of this paper are as follows:

- We propose a new joint communication and control algorithm for mmWave beam alignment method at BS for CAV in V2X networks, where both transmission data rate requirement in communications and event-triggered control policy are jointly considered in beam alignment

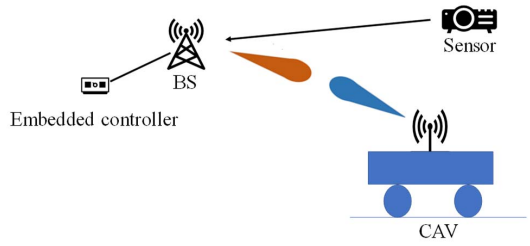

Fig. 1: Cellular assisted motion control of CAV with mmWave communications.

design. In return, such a beam alignment design can both guarantee high rate requirement of CAV and provide cellular assisted motion control to enhance safe driving of CAV.

- We analyze the effect of sampled information at the sensor from control perspective on the beam alignment in mmWave communications. A theorem is obtained to show the relationship between misalignment error and state error kept in the controller at BS, where the misalignment error follows Rayleigh distribution introduced because of the state error following Gaussian distribution.
- We discuss the effect of the beam misalignment on event-triggered cellular assisted motion control design, where the channel capacity loss introduced by misalignment is adopted as the event to trigger the cellular assisted motion control of CAV. Here, a closed-form expression of the channel capacity is obtained as control triggering threshold.

The rest of this paper is organized as follows. In Section II, the system model and problem statement are presented. In Section III, joint communication and control for mmWave beam alignment scheme is introduced. In Section IV, we analyze the stability performance of the proposed method. In Section V, simulation results are provided to show the performance. Finally, Section VI concludes the paper.

II. System Model and Problem Statement

In this section, we provide the system model by taking both mmWave communications and cellular assisted motion control of CAV into consideration. For the convenience of discussion, we consider a simplified CAV model as shown in Fig. 1. In Fig. 1, we only focus on the data transmission via the downlink, i.e., a BS transmitting the necessary data to a mobile CAV with constrained data rate via mmWave communications[1], where beam alignment is critical for the transmission. In fact, the transmission from a sensor to BS is also conducted by mmWave communications. The beam alignment is easy for the transmission from the sensor to BS since the sensor is deployed statically along the road. Since we focus on the beam alignment for the transmission from BS to CAV, the transmission from the sensor to BS is assumed perfect, i.e., there is no packet loss from the sensor to BS, to simplify our discussion, where the imperfect transmission would be treated as our future work. Here, the alignment of the transmitting beam of BS and the detection beam of the receiver is one of the most important parameters that determine the transmissions data rate from BS to CAV. In addition, a sensor[2] takes samples of CAV and sends them to BS when the transmission to CAV is activated by event-triggered policy. Then, a controller embedded in BS calculates a control command based on the received samples and sends it to CAV to update the state of CAV. Similar simplified motion control model for CAV has been adopted in many works [30]–[32]. In the following of this section, we first introduce the cellular assisted motion control model of CAV. Then, we present the mmWave communication model from BS to CAV. Finally, we provide the transmission activation problem from BS to CAV in event-triggered control policy. By solving the problem, The transmission data rate requirement from BS to CAV can be guaranteed with the proposed beam alignment method.

A. Cellular Assisted Motion Control Model

In the aforementioned control process, the discrete time motion control update function of CAV is given by [30]–[34]

$$\mathbf{x}_{k+1} = \mathbf{A}\mathbf{x}_k + \mathbf{B}u_k + \mathbf{w}_k, \tag{1}$$

where $\mathbf{x}_{k+1}$ is the updated state of CAV at time index $k+1$, $\mathbf{x}_k$ is the current sampled state of CAV at time index k, u_k is the motion control input, and $\mathbf{w}_k$ is the disturbance caused by additive white gaussian noise (AWGN) with zero mean and variance $\mathbf{W}$. In addition, $\mathbf{A}$ and $\mathbf{B}$ represent the system parameter matrices, which will be introduced later.

To illustrate such a model, an example of a cart with an inverted pendulum is adopted, where the goal of the cart's motion control is to maintain the balance of the inverted pendulum.

Example: To maintain the balance of the inverted pendulum, the controller needs the information about the cart's position and velocity and the pendulum's angle and angle velocity from the sensor. Then, the controller can calculate the control command for the cart to maintain the pendulum's balance. In the aforementioned motion control process, the state of the cart and inverted pendulum at time index k can be expressed as $\mathbf{x}_k = (c_k, \dot{c}_k, \theta_k, \dot{\theta}_k)$, where c_k represents the cart's position, $\dot{c}_k$ represents the cart's velocity, θ_k represents the pendulum's angle, and $\dot{\theta}_k$ represents the pendulum's angular velocity. Then, the expression of $\mathbf{A}$ and $\mathbf{B}$ consists of the pendulum length 2ξ, the inertia of the pendulum Ψ, the friction of the cart ζ, the gravitational acceleration ϕ, the mass

[1]Note that the scenario that mmWave blockage happens between BS and CAV would be treated as our future work.

[2]Here, we consider the sensor is independently deployed from BS and CAV, which is necessary for CAV to obtain global information for autonomous driving. Note that the sensor can also be embedded in CAV or BS can work as radar sensing the necessary information for autonomous driving.

of the pendulum λ, and the mass of the cart Λ. By physical-mathematics calculation, $\mathbf{A}$ and $\mathbf{B}$ can be expressed as [33]

$$\mathbf{A} = \begin{pmatrix} 0 & 1 & 0 & 0 \\ 0 & \frac{-(\Psi+\lambda\xi^2)\zeta}{\Psi(\Lambda+\lambda)+\Lambda\lambda\xi^2} & \frac{\lambda^2 g\xi^2}{\Psi(\Lambda+\lambda)+\Lambda\lambda\xi^2} & 0 \\ 0 & 0 & 0 & 1 \\ 0 & \frac{-\lambda\xi\zeta}{\Psi(\Lambda+\lambda)+\Lambda\lambda\xi^2} & \frac{\lambda\phi\xi(\Lambda+\lambda)}{\Psi(\Lambda+\lambda)+\Lambda\lambda\xi^2} & 0 \end{pmatrix}$$

and

$$\mathbf{B} = \begin{pmatrix} 0 \\ \frac{(\Psi+\lambda\xi^2)\zeta}{\Psi(\Lambda+\lambda)+\Lambda\lambda\xi^2} \\ 0 \\ \frac{\lambda\xi}{\Psi(\Lambda+\lambda)+\Lambda\lambda\xi^2} \end{pmatrix}.$$

More details about this example can be found in [35]. The pair $(\mathbf{A}, \mathbf{B})$ is assumed to be controllable and the initial state $\mathbf{x}_0$ is assumed to be given and determinate [36]. Substituting the above parameters into (1), we can obtain the discrete time motion control update function for the cart based inverted pendulum. ■

We assume that the sampled state at the sensor at each time index k is perfect and can be expressed as $\mathbf{y}_k = \mathbf{x}_k$. Such assumption is usually adopted in motion control research [30]–[34]. Furthermore, we assume that $\delta_k = 1$ represents that the sensor transmits the sampled state to the controller at BS at time index k and $\delta_k = 0$ represents that the transmission from the sensor to the controller is not activated. Then, the received the state information $\mathbf{z}_k$ at the controller from the sensor can expressed as

$$\mathbf{z}_k = \begin{cases} \mathbf{y}_k, & \text{when } \delta_k = 1, \\ \emptyset, & \text{when } \delta_k = 0. \end{cases} \tag{2}$$

Based on (2), the controller at BS can calculate the control input as

$$u_k = \mathbf{K}\mathbf{z}_k, \tag{3}$$

where $\mathbf{K}$ is the control gain.

B. mmWave Communication Model

We assume that the sensor are deployed along the road statically, where it is very easy to deal with beam alignment of the link from the sensor to BS[3]. Then, in this paper, we would focus the beam alignment of the downlink from BS to CAV in mmWave communications, which is used to guarantee the required ultra-high data rate of CAV and assist the motion control by the control command from the controller at BS to CAV. In the following of this subsection, we first introduce the signal model and channel capacity of the downlink via mmWave communications. Then, we provide the channel model of the downlink, especially the misalignment channel fading.

[3]The case that the sensor embedded in the vehicle is treated as our future work.

1) Signal Model: The received signal can be expressed as

$$y = hx + n, \tag{4}$$

where $x \in \mathbb{C}$ is the complex transmitted signal, $h \in \mathbb{C}$ is the complex flat fading wireless channel, $n \in \mathbb{C}$ is complex additive noise with zero-mean and variance N_0, i.e., $n \backsim CN(0, N_0)$. Then, the channel capacity can be obtained as

$$C = \log_2(1+\gamma) = \log_2(1 + \frac{|h|^2 P}{N_0}), \tag{5}$$

where P is the transmission power.

2) Channel Model: The flat fading wireless channel h in (4) consists of path-loss h_g, multipath fading h_f, and misalignment fading h_m, which can be expressed as

$$h = h_g h_f h_m. \tag{6}$$

Next, we would introduce them in details, respectively.

- Path-loss: The path-loss h_g in mmWave communications consists of propagation loss h_{gp} and molecular absorption h_{ga}, which can be expressed as

$$h_g = h_{gp} h_{ga}. \tag{7}$$

In (7), the propagation loss h_{gp} can be obtained by

$$h_{gp} = \frac{c\sqrt{G_t G_r}}{4\pi f d}, \tag{8}$$

where G_t and G_r are the transmission and reception gains depending on antenna orientation, respectively. In addition, c is the speed of light, f is the occupied frequency band, and d is the distance between transceiver. Furthermore, the molecular absorption h_{ga} can be expressed as [37]

$$h_{ga} = e^{-\frac{1}{2}\kappa_\alpha(f)d}, \tag{9}$$

where $\kappa_\alpha(f)$ is the medium absorption factor for the relative area per unit of volume. For the convenience of discussion, a simplified medium absorption factor model in [9] is adopted in this paper, which is expressed as

$$\kappa_\alpha(f) = \varphi_1(f, v) + \varphi_2(f, v) + \varphi_3(f). \tag{10}$$

According to [9], we have

$$\varphi_1(f, v) = \frac{\Psi_1(v)}{\Omega_1(v) + (\frac{f}{100c} - c_1)^2}, \tag{11}$$

$$\varphi_2(f, v) = \frac{\Psi_2(v)}{\Omega_2(v) + (\frac{f}{100c} - c_2)^2}, \tag{12}$$

and

$$\varphi_3(f) = p_1 f^3 + p_2 f^2 + p_3 f + p_4. \tag{13}$$

According to [37], we have $c_1 = 10.835$ cm^{-1}, $c_2 = 12.664$ cm^{-1}, $p_1 = 5.54\times10^{-37}$ Hz^{-3}, $p_2 = -3.94\times10^{-25}$ Hz^{-2}, $p_3 = 9.06\times10^{-14}$ Hz^{-1}, $p_4 = -6.36\times10^{-3}$. In addition, $\Psi_1(v) = g_1 v(g_2 v + g_3)$, $\Omega_1(v) = (g_4 v + g_5)^2$, $\Psi_2(v) = g_5 v(g_6 v + g_7)$, and $\Omega_2(v) = (g_8 v + g_9)^2$, where $g_1 = 0.2205$, $g_2 = 0.1303$, $g_3 = 0.0294$, $g_4 = 0.4093$, $g_5 = 0.0925$, $g_6 = 0.1702$, $g_7 = 0.0303$, $g_8 = 0.537$,

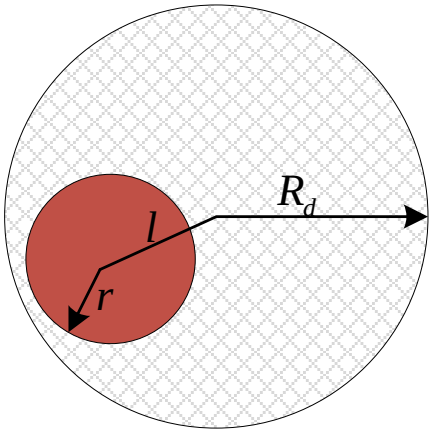

Fig. 2: Misalignment between BS beam and receiver beam.

and $g_9 = 0.0956$. Furthermore, v is the mixed ratio of water vapor in unit volume, which can be expressed as $v = (\rho p_w(T,p))/(100p)$. Here, ρ and p are relative humidity and atmospheric pressure, respectively, and $p_w(T,p)$ is the saturated water vapor partial pressure when the temperature is T. According to [9], we have

$$p_w(T,p) = q_1(q_2 + q_3\eta_h)e^{\frac{q_4(T-q_5)}{T-q_6}},$$

where $q_1 = 6.1121$, $q_2 = 1.0007$, $q_3 = 3.46\times10^{-6}$ hPa^{-1}, $q_4 = 17.502$, $q_5 = 273.15$ ^{0}K, $q_6 = 32.18$ ^{0}K, and η_h is the pressure in hPa

- Multipath fading: In this paper, we consider that the multipath fading is represented by Rayleigh distribution, where its probability distribution function (pdf) can be expressed by [37]

$$f_{h_f} = \frac{2}{\hat{h}_f^2\Gamma(1)}\cdot x\cdot e^{-\frac{x^2}{\hat{h}_f^2}}, \tag{14}$$

where $\hat{h}_f$ is the $\alpha = 2$ root mean value of the fading channel envelop.

- Misalignment fading: As shown in Fig. 2, We assume that the detection beam of the receiver covers an area of S with radius r and the radius of the covering area for the transmitting beam is R at distance d, where $0 \le R \le R_d$ and R_d is the maximum radius of the beam at distance d. In addition, l is the misalignment error between the beam center of the transceiver. Then, according to [38], the misalignment fading can be expressed as

$$h_m = S_0 e^{-\frac{2l^2}{R_{eq}^2}}, \tag{15}$$

which means that misalignment fading is represented by the power received at the receiver in the area S at distance d. In addition, R_{eq} is the equivalent beam-width and S_0 the received power when $l = 0$, which can be expressed as

$$S_0 = \mathrm{erf}(\epsilon)^2. \tag{16}$$

Here, we have $\epsilon = (\sqrt{\pi}r)/(\sqrt{2}R_d)$ and $\mathrm{erf}(\cdot)$ is Gauss error function. Furthermore, the equivalent beam-width R_{eq} can be expressed as

$$R_{eq}^2 = R_d^2\frac{\sqrt{\pi}\mathrm{erf}(\epsilon)}{2\epsilon e^{-\epsilon^2}}. \tag{17}$$

C. Problem Statement

Based on cellular assisted control model and mmWave communication model, we discuss how to jointly design communication and control to obtain the downlink transmission activation policy in (2). Such a design aims to obtain proper beam alignment area maintaining the data rate requirement in the downlink communications. Furthermore, this design should provide more time resource for data transmission than periodical time triggered motion control, and meanwhile guarantee control performance. According to [29], if there is no transmission from sensor to controller, the error between the known state at the controller and the actual state of CAV would increase. This would enlarge the misalignment distance l in Fig. 2. Then, the channel capacity will reduce significantly in mmWave communications. We assume that there is a capacity threshold C_{th} to guarantee the data rate requirement. Then, there should be a transmission activation design on δ_k to guarantee data rate requirement, which can be expressed as

$$\delta_k = \begin{cases} 1, & \text{if } C_k \le C_{th}, \\ 0, & \text{if } C_k > C_{th}, \end{cases} \tag{18}$$

where there is no need to activate the transmission when the data rate is larger than the threshold at time index k, i.e., $C_k > C_{th}$. Otherwise, the transmission is necessary when $C_k \le C_{th}$.

The goal of this paper is to find a proper threshold C_{th} for (18) to reduce wireless resource consumption at the sensor, maintain control performance, and meanwhile guarantee the channel capacity requirement in mmWave communications.

III. Joint Communication and Control for Beam Alignment Scheme

We intend to find a feasible control triggering policy to reduce the effect of beam misalignment on date rate loss in mmWave communications, as well as maintain control stability. Thus, in the following of this section, we first analyze the data rate loss introduced by beam misalignment. Then, we develop the control triggering condition constrained by data rate requirement. Since the position of the CAV affects the beam alignment, we only abstract the horizontal position of the cart and the vertical position of the inverted pendulum in the proposed scheme in the following of this paper.

A. Data Rate Loss Introduced by Beam Misalignment in mmWave Communications

From (5) and (6), the channel capacity can be further written as[4]

$$C = \log_2(1 + \frac{|h|^2P}{N_0}) = \log_2(1 + \frac{|h_g|^2|h_f|^2|h_m|^2P}{N_0}). \tag{19}$$

[4]Here, we omit the time index k since the capacity expression holds for each index k.

where h_g, h_f, and h_m are independent. In (19), path-loss h_g and Rayleigh fading h_f have no effect on beam misalignment. Next, we focus on beam misalignment fading coefficient h_m.

From (15), the misalignment fading is determined by the misalignment error l between the beam center of the transceiver, where the error l is further determined by wireless motion control triggered policy. Then, we can conclude that the data rate loss is determined by wireless motion control triggered policy. Specifically, when the received the state information $\mathbf{x}_k$ at the BS from the sensor is with high accuracy, the error l would be small. Then, the misalignment fading coefficient h_m is small, which leads to small data rate loss in (19). Otherwise, the data rate loss in (19) would be large.

B. Misalignment Distance Error Introduced by Motion Control

In this subsection, we intend to obtain a data rate requirement based method for control triggering policy. Since most sensors are power by battery, reducing energy consumption is very important for wireless control system design, where event-triggered methods are very popular to deal with this issue from control perspective. In such methods, the sensor is usually supposed to keep a local estimate of the state for triggering policy design[5] [29]. The estimated state can be written as[6]

$$\hat{\mathbf{x}}_{k+1|k} = \mathbf{A}\hat{\mathbf{x}}_{k|k} + \mathbf{B}u_k, \tag{20}$$

where $\mathbf{w}_k$ in (1) is omitted since it is random parameter at the vehicle and can not be predicted at the sensor [29]. Equation (20) means that the state estimation at time index $k+1$ is determined by the state estimation and the control input at the latest time index k. In addition, $\hat{\mathbf{x}}_{k|k}$ is the state estimation at time index k and can be expressed as

$$\hat{\mathbf{x}}_{k|k} = \begin{cases} \mathbf{x}_k, & \text{when } \delta_k = 1, \\ \hat{\mathbf{x}}_{k|k-1}, & \text{when } \delta_k = 0. \end{cases} \tag{21}$$

If the sensor can obtain the control triggering policy based on its estimation and observation to determine when it is necessary to transmit the observation to the BS, huge amount of energy consumption would be saved compared with transmitting at each time index k.

Jointly considering the actual control update in (1) and estimated state in (20), we can obtain the error between actual state and estimated state as

$$\mathbf{e}_{k+1} \triangleq \mathbf{x}_{k+1} - \hat{\mathbf{x}}_{k+1|k} = \sum_{i=0}^{n} \mathbf{A}^{n-i}\mathbf{w}_i, \tag{22}$$

where $i = 0, 1, 2, ..., n$ is the time step from k to $k+1$ that no transmission occurs. The equation (22) indicates that the error between the observation state $\mathbf{y}_{k+1} = \mathbf{x}_{k+1}$ and the estimated state at the sensor follows AWGN distribution. Then, each element in $\mathbf{e}_{k+1}$ of (22) can be expressed as

$$e_{k+1}^{(j)} = \sum_{i=0}^{n}\sum_{m=1}^{M} \mathbf{A}_{j,m}^{n-i}\mathbf{w}_i^{(m)}, \tag{23}$$

where j and $m = 1, ..., M$ are the row and column of $\mathbf{A}$. Then, $\mathbf{e}_{k+1}$ follows AWGN distribution with zero mean and variance

$$\Delta = [\sigma_{x_1}^2, \sigma_{x_2}^2]^T = (\sum_{i=0}^{n} \mathbf{A}^{n-i})^2\mathbf{W}.$$

From communication perspective, to obtain the misalignment error, we need the position information in the state $\mathbf{x}_{k+1}$, where the horizontal position is represented as $x_{1,k+1}$ and the vertical position is represented as $x_{2,k+1}$, respectively. We further assume that $\sigma^2 = \sigma_{x_1}^2$ and $\tau^2 = \sigma_{x_2}^2/\sigma_{x_1}^2$. Then, we have the following theorem of the error[7] $l = \sqrt{x_1^2 + x_2^2}$.

Theorem 1. The misalignment error $l = \sqrt{x_1^2 + x_2^2}$ between the beam center of the transceiver follows Rayleigh distribution, where its pdf can be expressed as

$$f_l(l) = \frac{l}{\sigma_s^2}\exp(-\frac{l^2}{2\sigma_s^2}), \tag{24}$$

where the mean is $\mathbb{E}(l) = \frac{\tau\sigma}{2\sqrt{2\pi}}E(2\pi|1-\frac{1}{\tau}|)$ and the variance is $\text{var}(l) = \frac{4-\pi}{2}\left(\frac{\tau\sigma}{2\pi}E(2\pi|1-\frac{1}{\tau}|)\right)^2$. Here, $E(2\pi|1-\frac{1}{\tau}|)$ is the elliptic integral of the second kind.

Proof. See Appendix A.

C. Control Triggering Policy Constrained by Data Rate Requirement

Next, we discuss the threshold C_{th} design and obtain a closed-form expression for C_{th}.

From (15) and (19), we have

$$\begin{aligned} C_k &= \log_2(1 + |h_g|^2|h_f|^2|S_0 e^{-\frac{2l^2}{R_{eq}^2}}|^2\frac{P}{N_0}) \\ &= \log_2\left(1 + a(\exp(bl_k^2))^2\right), \end{aligned} \tag{25}$$

where $a = S_0^2|h_g|^2|h_f|^2\frac{P}{N_0}$ and $b = -\frac{2}{R_{eq}^2}$. Based on (24), we can obtain the pdf of the channel capacity as

$$f_{C_k}(c) = \frac{-2^c\ln(2)}{4b\sigma_s^2(2^c-1)}\left(\frac{2^c-1}{a}\right)^{\frac{-1}{4b\sigma_s^2}} \tag{26}$$

Given control triggering probability p_{tr}, we have

$$\begin{aligned} p_{tr} &= \Pr\{C_k \le C_{th}\} \\ &= \int_{-\infty}^{C_{th}} \frac{-2^c\ln(2)}{4b\sigma_s^2(2^c-1)}\left(\frac{2^c-1}{a}\right)^{\frac{-1}{4b\sigma_s^2}} dy \\ &= \left(\frac{2^{C_{th}}-1}{a}\right)^{\frac{-1}{4b\sigma_s^2}}. \end{aligned} \tag{27}$$

Then, the triggering threshold of the mmWave communications for motion control can be expressed as

$$C_{th} = \log_2(ap_{tr}^{-4b\sigma_s^2} + 1). \tag{28}$$

[5]Note that the Kalman filter estimating states from control perspective is not recommended to be used at the sensor since the limited available energy and computing property.

[6]This estimation method belongs to model predictive control method, which is widely used at the sensor.

[7]Here, we omit the time index k since the expression of the error holds for each index k.

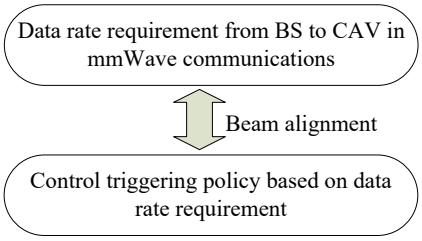

Fig. 3: Relationship in joint communication and control design for beam alignment in mmWave communications for CAV.

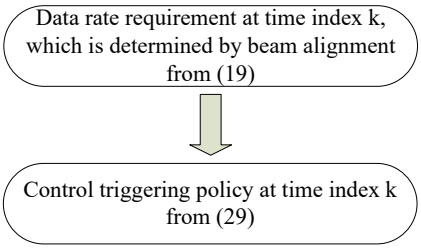

Fig. 4: Operating process of the proposed method.

Finally, the control triggering condition can be rewritten as

$$\delta_k = \begin{cases} 1, & \text{if } \ C_k \le \log_2(a p_{tr}^{-4b\sigma_s^2} + 1), \\ 0, & \text{if } \ C_k > \log_2(a p_{tr}^{-4b\sigma_s^2} + 1). \end{cases} \tag{29}$$

In (29), this paper obtains a threshold C_{th} at each time index k with closed-form expression, which reduce wireless resource consumption at the sensor and meanwhile guarantee the channel capacity requirement in mmWave communications.

In Fig. 3, we conclude the proposed joint communication and control design for beam alignment in mmWave communications for CAV. From this figure, the beam alignment in mmWave communications links the data rate in mmWave communications and control triggering policy design. On the one hand, the beam alignment is one of the most important parameters that determine the transmission data rate in mmWave communications. The data rate would experience large loss if the beam misalignment is large. Furthermore, the data rate requirement would bring a constraint on beam alignment. When the beam alignment is in a certain range, the data rate requirement can be guaranteed. On the other hand, the beam alignment is determined by the control state error of CAV. Theorem 1 shows that large state error would increase the beam misalignment. In addition, the successful control state update is determined by beam alignment. If the beam misalignment is too large to support the control command transmission from BS to CAV, the state error would be enlarged. Then, the transmission data rate requirement cannot be guaranteed. Thus, the control state update could be failed because of communication packet loss. In summary, we obtain (29) to indicate the joint communication data rate and control triggering policy design for beam alignment for CAV in V2X networks. In (29), by setting a data rate threshold in data transmission from BS to CAV guaranteeing control requirement and communication requirement, the proposed control triggering policy can be obtained for beam alignment in mmWave communications.

In Fig. 4, we conclude the operating process of the proposed method. First, the data rate requirement at each time index k determined by beam alignment can be obtained by (19), which is treated as the threshold of data rate at the time index k. Then, based on (29), we can obtain that whether the control update of CAV should be triggered or not.

In the next section, we provide the control performance of the proposed method, which will show that the control stability can be maintained by the proposed method.

IV. Control Stability Analysis of The Proposed Method

In this section, we discuss the stability performance of the proposed method, where we focus on the mean-square stability. We assume that the control input is represented by

$$u_k = \mathbf{K}\hat{\mathbf{x}}_{k|k}, \tag{30}$$

where $\mathbf{K} = -(\mathbf{R} + \mathbf{B}^T\mathbf{P}\mathbf{B})^{-1}\mathbf{B}^T\mathbf{P}\mathbf{A}$ [29]. Here, $\mathbf{P}$ is the unique positive definite solution to the following algebraic Riccati equation, i.e., $\mathbf{P} = \mathbf{A}^T\mathbf{P}\mathbf{A} + \mathbf{Q} - \mathbf{K}^T(\mathbf{R} + \mathbf{B}^T\mathbf{P}\mathbf{B})\mathbf{K}$, where $\mathbf{R} \in R^{m\times m}$ is positive definite, $\mathbf{Q} \in R^{n\times n}$ is positive semi-definite, and matrix pair $(\mathbf{A}, \mathbf{Q}^{\frac{1}{2}})$ is observable.

Let $k_0 = 0$, $\delta_{k_0} = 1$, $k_{j+1} = \inf\{k' \in \{k_j+1, \cdots, k-1\} | \delta_{k'} = 1\}$, $i = \max\{j \in N | k_j < k\}$. Then, we have $j \in \{1, 2, \cdots, i\}$, which means that i transmissions occur in k time indexes and the transmission time index is k_j. Then, (22) can be further rewritten as

$$\mathbf{x}_{k_j} = (\mathbf{A} + \mathbf{B}\mathbf{K})^{k_j - k_{j-1}}\mathbf{x}_{k_{j-1}} + \sum_{m=k_{j-1}}^{k_j-1} \mathbf{A}^{k_j-1-m}\mathbf{w}_m. \tag{31}$$

Furthermore, we have mean-square expression as

$$\mathbb{E}[\mathbf{x}_{k_j}^T\mathbf{x}_{k_j}] = \mathrm{Tr}\big(\mathbb{E}[\mathbf{x}_{k_j}\mathbf{x}_{k_j}^T]\big), \tag{32}$$

where $\mathrm{Tr}(\cdot)$ is the trace operation. In the following, we discuss $\mathbb{E}[\mathbf{x}_{k_j}\mathbf{x}_{k_j}^T]$ in (32), which can be expressed as (33) on the top of next page. We assume

$$\mathbf{G}_{k_j} = \mathbb{E}\Big[\Big(\sum_{m=k_{j-1}}^{k_j-1} \mathbf{A}^{k_j-1-m}\mathbf{w}_m\Big)\Big(\sum_{m=k_{j-1}}^{k_j-1} \mathbf{A}^{k_j-1-m}\mathbf{w}_m\Big)^T\Big]. \tag{34}$$

Then, we have the relationship between $\mathbf{x}_{k_j}$ and $\mathbf{x}_0$ as

$$\begin{aligned} \mathbb{E}[\mathbf{x}_{k_j}\mathbf{x}_{k_j}^T] &= (\mathbf{A} + \mathbf{B}\mathbf{K})^{k_j}\mathbf{x}_0\mathbf{x}_0^T((\mathbf{A} + \mathbf{B}\mathbf{K})^{k_j})^T \\ &+ \sum_{m=1}^{i}(\mathbf{A} + \mathbf{B}\mathbf{K})^{k_j-k_m}G_{k_m}((\mathbf{A} + \mathbf{B}\mathbf{K})^{k_j-k_m})^T, \end{aligned} \tag{35}$$

where the second term on the right side is bounded since $\mathbf{x}_0$ is constant. Then, we need to show that the first term on the right side is bounded. Since $\mathbf{w}_m$ is independent identically distributed (i.i.d), we can obtain

$$\mathbf{G}_{k_j} = \sum_{m=k_{j-1}}^{k_j-1} \mathbf{A}^{k_j-1-m}\mathbf{W}(\mathbf{A}^{k_j-1-m})^T, \tag{36}$$

$$\mathbb{E}[\mathbf{x}_{k_j}\mathbf{x}_{k_j}^T] = \mathbb{E}\Big[\Big(\sum_{m=k_{j-1}}^{k_j-1} A^{k_j-1-m}w_m\Big)\Big(\sum_{m=t_{j-1}}^{k_j-1} A^{k_j-1-m}w_m\Big)^T\Big] + \mathbb{E}\Big[(A+BK)^{k_j-k_{j-1}}\mathbf{x}_{k_{j-1}}\mathbf{x}_{k_{j-1}}^T\big((A+BK)^{k_j-k_{j-1}}\big)^T\Big], \tag{33}$$

where the zero mean value of w_m is adopted.

which means that the the total noise power is the accumulation of the failed transmission time indexes from the latest successful transmission.

We assume that $\mathrm{Tr}(\mathbf{W}) < d$. Then, $\mathrm{Tr}(\mathbf{G}_{k_j})$ is bounded, where there exists a positive definite matrix $\mathbf{S}$ that makes the following expression hold, i.e.,

$$\mathbf{G}_{k_j} \le \mathbf{S} - (\mathbf{A}+\mathbf{BK})\mathbf{S}(\mathbf{A}+\mathbf{BK})^T. \tag{37}$$

Then, for each time index k, we have (38) on the top of next page.

From (32) and (38), we can obtain

$$\mathbb{E}[\mathbf{x}_{k_j}^T\mathbf{x}_{k_j}] \le \mathrm{Tr}(\mathbf{S}) + \mathbf{x}_0^T\left((\mathbf{A}+\mathbf{BK})^k\right)^T(\mathbf{A}+\mathbf{BK})^k\mathbf{x}_0. \tag{39}$$

We assume that there exists $\mu \in [0,1)$ satisfying $(\mathbf{A}+\mathbf{BK})^T\mathbf{P}(\mathbf{A}+\mathbf{BK}) \le \mu\mathbf{P}$. Then, (39) can be further written as

$$\begin{aligned}\mathbb{E}[\mathbf{x}_{k_j}^T\mathbf{x}_{k_j}] &\le \mathrm{Tr}(\mathbf{S}) + \mathbf{x}_0^T\left((\mathbf{A}+\mathbf{BK})^k\right)^T(\mathbf{A}+\mathbf{BK})^k\mathbf{x}_0 \\ &\le \mathrm{Tr}(\mathbf{S}) + \frac{\lambda_{\max}(\mathbf{P})}{\lambda_{\min}(\mathbf{P})}\mu^k\mathbf{x}_0^T\mathbf{x}_0,\end{aligned} \tag{40}$$

which means that the mean-square of $\mathbb{E}[\mathbf{x}_{k_j}^T\mathbf{x}_{k_j}]$ is upper bounded. In other word, the adopted wireless control system of the proposed method is mean-square stable. Then, we can conclude that the proposed method can reduce wireless resource consumption at the sensor, maintain control stability, and meanwhile guarantee the channel capacity requirement in mmWave communications.

V. Simulation Results

In this section, we provide simulation results of both mmWave communications and motion control of CAV to demonstrate the performance of the proposed method, where the system model is the same as shown in Fig. 1. For simplicity, only the horizontal and vertical positions of the inverted pendulum with cart are considered, where we assume that $\mathbf{A} = \begin{bmatrix}1 & 1\\ 0 & 1\end{bmatrix}$, $\mathbf{B} = (0.5,1)^T$, $\mathbf{w}_k \sim N(0, 0.5)$, and control input gain is $\mathbf{K} = (-0.2068, -0.6756)^T$. Furthermore, the activation probability of the sensor is $p_{tr} = 0.33$, transmission SNR is $P/N_0 = 25$ dB, the radius of the beam for the receiver antenna is $r = 0.85$, the radius of the beam for the BS antenna is $R_d = 0.55$, and the multipath fading is $h_f = 1$. In addition, the periodical time triggered control method in [39] is adopted as the benchmark to show the performance of the proposed method in this paper.

Fig. 5 demonstrates the CAV state update with different sampling time index, where the triggering probability is $P_{tr} = 0.35$ and $\|\mathbf{x}_k\|_2 = \sqrt{x_{1,k}^2 + x_{2,k}^2}$ is the 2-norm of the state $\mathbf{x}_k$. From this figure, both the conventional periodical time triggered method and the proposed joint communication and control algorithm for mmWave beam alignment method with capacity threshold triggered control would maintain stable with sampling time index increasing, e.g., the state would be stable when $k \ge 9$ in this figure. In addition, the difference of the control performance for the conventional method and the proposed method is minor, which indicates that the proposed method works well from control perspective.

Fig. 6 shows the cumulative probability of the total triggering numbers in control process, where 500 control time indexes are counted in the control process. From this figure, compared with the conventional periodical time triggered method, the proposed method can significantly reduces the total transmission frequency and meanwhile guarantee the rate requirement at each sampling time index.

Fig. 7 illustrates the statistical channel capacity performance of the proposed method, i.e., cumulative distribution function (CDF) of channel capacity, where the triggering probability is $P_{tr} = 0.35$. From this figure, the statistical channel capacity performance of the proposed method is similar to the conventional method with minor performance loss.

Fig. 8 shows the channel capacity performance of the proposed method when the triggering probability of the sensor increases. From this figure, the channel capacity of the proposed method increases with triggering probability increasing. This is reasonable since larger triggering probability leads to larger transmission frequency, which further reduces the error between estimated position and actual position of the CAV. When triggering probability is large enough, e.g., $p_{tr} \ge 0.32$ in this figure, the channel capacity loss of the proposed method can be ignored compared with convention method. In addition, we provide the GPS-based motion control prediction method for beam alignment in [28] as the comparison. Compare with the adopted method in [28], the proposed method in this paper can achieve significant high channel capacity with larger probability. This is reasonable since the proposed method in this paper is based on the actual kinematic model of CAV, which can provide high prediction precision compared with GPS-based motion control prediction. Then, the beam alignment is more accuracy than that in [28], which leads to higher data rate than that in [28].

In summary, the simulation results indicate that the proposed joint communication and control for mmWave beam alignment method with capacity threshold triggered control can guarantee the rate requirement of the CAV in mmWave communications for future V2X networks and meanwhile maintain good cellular assisted motion control performance of the CAV.

$$\begin{aligned}
&\mathbb{E}[\mathbf{x}_{k_j}\mathbf{x}_{k_j}^T] = \mathbb{E}\big[(\sum_{m=k_i}^{k-1}\mathbf{A}^{k-1-m}w_m)(\sum_{m=k_i}^{k-1}\mathbf{A}^{k-1-m}w_m)^T\big] \\
&+\sum_{m=1}^{i}(\mathbf{A}+\mathbf{BK})^{k-k_m}\mathbf{G}_{k_m}(\sum_{m=1}^{i}(\mathbf{A}+\mathbf{BK})^{k-k_m})^T + (\mathbf{A}+\mathbf{BK})^k\mathbf{x}_0\mathbf{x}_0^T((\mathbf{A}+\mathbf{BK})^k)^T \\
&\le \mathbf{G}_k + (\mathbf{A}+\mathbf{BK})^k\mathbf{x}_0\mathbf{x}_0^T((\mathbf{A}+\mathbf{BK})^k)^T + \sum_{m=1}^{i}(\mathbf{A}+\mathbf{BK})^{k-k_m}\mathbf{G}_{k_m}(\sum_{m=1}^{i}(\mathbf{A}+\mathbf{BK})^{k-k_m})^T \\
&\le \mathbf{S} + (\mathbf{A}+\mathbf{BK})^k\mathbf{x}_0\mathbf{x}_0^T((\mathbf{A}+\mathbf{BK})^k)^T.
\end{aligned} \tag{38}$$

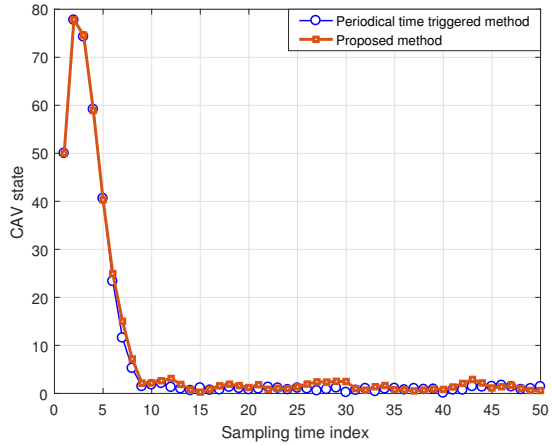

Fig. 5: CAV control performance with sampling time index.

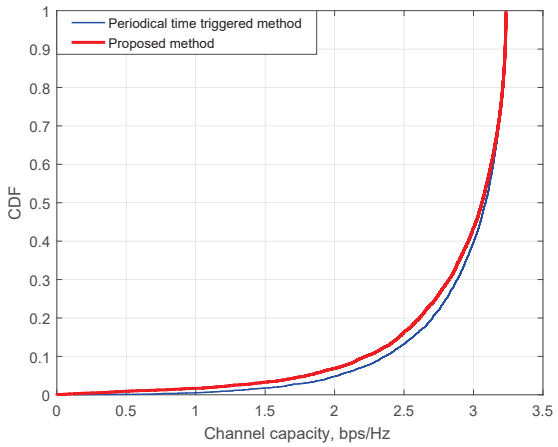

Fig. 7: CDF performance of the channel capacity for the proposed method.

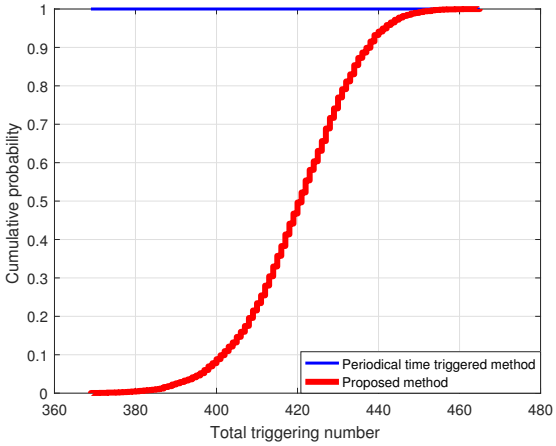

Fig. 6: Cumulative probability of the total triggering numbers in control process.

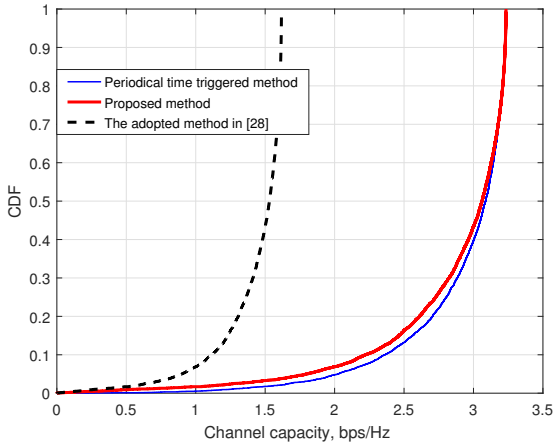

Fig. 8: Channel capacity with different triggering probability.

VI. Conclusions

In this paper, we proposed a new joint communication and control algorithm for beam alignment, where the mutual positive effect of mmWave/THz communications and motion control of CAV on each other is discussed. First, we provided a framework to show the interaction between motion control of CAV and beam alignment of mmWave/THz communications. Second, we analyzed the effect of CAV control on beam alignment in mmWave/THz communications, where the closed-form expression of their relationship is obtained. Third, we discussed the CAV control design affected by beam alignment. Finally, we obtained the control stability performance of the proposed method. Simulation results indicated that the proposed method could guarantee the rate requirement of the CAV in mmWave/THz communications in V2X networks and meanwhile maintained good cellular assisted motion control

performance of the CAV.

APPENDIX A

This appendix provides the detailed proof of Theorem 1.

According to [37], the envelope of the sum of two independent Gaussian signal follows Rayleigh distribution. Then, we have the misalignment error $l = \sqrt{x_1^2 + x_2^2}$ between the beam center of the transceiver follows Rayleigh distribution. Since x_1 and x_2 are independent, we can obtain

$$f(x_1, x_2) = \frac{1}{2\pi\tau\sigma^2} \exp(-\frac{1}{2\sigma^2}(x_1 + \frac{x_2^2}{\tau^2})). \tag{41}$$

Then, the mean can be expressed as

$$\mathbb{E}(\sqrt{x_1^2 + x_2^2}) = \int \int \sqrt{x_1^2 + x_2^2} f(x_1, x_2) dx_1 dx_2. \tag{42}$$

We assume $x_1 = q\cos(\lambda)$ and $x_2 = q\sin(\lambda)$. Then, (42) can be further written as

$$\begin{aligned} &\mathbb{E}(\sqrt{x_1^2 + x_2^2}) = \frac{1}{2\pi\tau\sigma^2} \int_0^{2\pi} \int_0^{+\infty} \\ &q^2 \exp(-\frac{q^1}{2\sigma^2}(\cos^2(\lambda) + \frac{\sin^2(\lambda)}{\tau^2})) dq d\lambda \\ &= \frac{\tau\sigma}{2\sqrt{2\pi}} E(2\pi|1 - \frac{1}{\tau}), \end{aligned} \tag{43}$$

where $E(2\pi|1 - \frac{1}{\tau})$ is the elliptic integral of the second kind. Then, we have in σ_s in (24) as

$$\sigma_s = \frac{\tau\sigma}{2\pi} E(2\pi|1 - \frac{1}{\tau}) \tag{44}$$

Then, the pdf can be written as

$$\begin{aligned} &f_l(l) = \frac{l}{\sigma_s^2} \exp(-\frac{l^2}{2\sigma_s^2}) \\ &= \frac{l}{(\frac{\tau\sigma}{2\pi} E(2\pi|1 - \frac{1}{\tau}))^2} \exp(-\frac{l^2}{2(\frac{\tau\sigma}{2\pi} E(2\pi|1 - \frac{1}{\tau}))^2}). \end{aligned} \tag{45}$$

The proof for Theorem 1 is completed.

REFERENCES

[1] J. He, K. Yang, and H. Chen, "6G cellular networks and connected autonomous vehicles," *IEEE Network*, early access, pp. 1-7, Nov. 2020.

[2] H. Zhou, W. Xu, J. Chen, and W. Wang, "Evolutionary V2X technologies toward the internet of vehicles: challenges and opportunities," *Proc. IEEE*, vol. 108, no. 2, pp. 308-323, Feb. 2020.

[3] E. Uhlemann, "Time for autonomous vehicles to connect [connected vehicles]," *IEEE Veh. Tech. Mag.*, vol. 13, no. 3, pp. 10–13, Sept. 2018.

[4] Intel, *Data is the new oil in the future of automated driving*. Nov. 2016.

[5] F. Gutierrez, "State of the art in 60-GHz integrated circuits and systems for wireless communications," *Proc. IEEE*, vol. 99, no. 8, pp. 1390-1436, Aug. 2011.

[6] G. Zhao, M. A. Imran, Z. Pang, Z. Chen, and L. Li, "Toward real-time control in future wireless networks: communication-control co-design," *IEEE Commun. Mag.*, vol. 57, no. 2, pp. 138-144, Feb. 2019.

[7] X. Wang et al., "Millimeter wave communication: a comprehensive survey," *IEEE Commun. Surveys Tuts.*, vol. 20, no. 3, pp. 1616-1653, 3rd Quart., 2018.

[8] P. Liu, J. Blumenstein, N. S. Perović, M. D. Renzo, and A. Springer, "Performance of generalized spatial modulation MIMO over measured 60GHz indoor channels," *IEEE Trans. Commun.*, vol. 66, no. 1, pp. 133-148, Jan. 2018.

[9] Z. Chen, et al., "A survey on terahertz communications," *China Commun.*, vol. 16, no. 2, pp. 1-35, Feb. 2019.

[10] B. Ning, Z. Chen, W. Chen, Y. Du, and J. Fang, "Terahertz multi-user massive MIMO with intelligent reflecting surface: beam training and hybrid beamforming," *IEEE Trans. Veh. Tech.*, vol. 70, no. 2, pp. 1376-1393, Feb. 2021.

[11] S. A. Busari, et al., "Generalized hybrid beamforming for vehicular connectivity using THz massive MIMO," *IEEE Trans. Veh. Tech.*, vol. 68, no. 9, pp. 8372–83, Sept. 2019.

[12] C. Chaccour, M. Naderi Soorki, W. Saad, M. Bennis, and P. Popovski, "Can terahertz provide high-rate reliable low latency communications for wireless VR?" 2020, *arXiv:2005.00536*. [Online]. Available: http://arxiv.org/abs/2005.00536

[13] C. Han and Y. Chen, "Propagation modeling for wireless communications in the terahertz band," *IEEE Commun. Mag.*, vol. 56, no. 6, pp. 96-101, Jun. 2018.

[14] S. Mumtaz, et al., "Cognitive vehicular communication for 5G," *IEEE Commun. Mag.*, vol. 53, no. 7, pp. 109-117, Jul. 2015.

[15] S. Mumtaz, S. Huq, K. Mohammed, and J. Rodriguez, "Direct mobile-to-mobile communication: Paradigm for 5G," *IEEE Wireless Commun.*, vol. 21, no. 5, pp. 14–23, Oct. 2014.

[16] L. Dai, Z. Wang, and Z. Yang, "Spectrally efficient time-frequency training OFDM for mobile large-scale MIMO systems," *IEEE J. Sel. Areas Commun.*, vol. 31, no. 2, pp. 251–263, Feb. 2013.

[17] H. Li, C. Li, H. Gao, S. Wu, and G. Fang "Study of moving targets tracking methods for a multi-beam tracking system in terahertz band," *IEEE Sensors J.*, accepted, pp. 1-10, Nov. 2020.

[18] "IEEE 802.11ad - Enhancements for Very High Throughput in the 60 GHz Band," no. 3, Mar. 2014.

[19] I. Aykin and M. Krunz, "Efficient beam sweeping algorithms and initial access protocols for millimeter-wave networks," *IEEE Trans. Wireless Commun.*, vol. 19, no. 4, pp. 2504-2514, Apr. 2020.

[20] Z. Wei, et al., "A two-stage beam alignment framework for hybrid MmWave distributed antenna systems," in Proc. *IEEE Int. Workshop Signal Process. Adv. Wireless Commun.*, Jul. 2019, pp. 1–5.

[21] V. Petrov, et al., " On unified vehicular communications and radar sensing in millimeter-wave and low terahertz bands" *IEEE Wireless Commun.*, vol. 26, no. 3, pp. 146-153, Jun. 2019.

[22] J. Li, Q. Zeng, R. Liu, and T. A. Denidni, "A compact dual-band beam-sweeping antenna based on active frequency selective surfaces," *IEEE Trans. Antennas and Propagation*, vol. 65, no. 4, pp. 1542-1549, Apr. 2017

[23] A. Mazin, M. Elkourdi, and R. D. Gitlin, "Accelerating beam sweeping in mmWave standalone 5G new radios using recurrent neural networks," in Proc. *IEEE 88th Veh. Technol. Conf. (VTC-Fall)*, Aug. 2018, pp. 1-4.

[24] J. Zhang, X. Chen, M. Li, and M. Zhao, "Optimized throughput in covert millimeter-wave UAV communications with beam sweeping," *IEEE Wireless Commun. Lett.*, early access, pp. 1-4, Dec. 2020

[25] V. Desai, et al., "Initial beamforming for mmWave communications," in Proc. *48th Asilomar Conf. Signals, Syst. Comput.*, Nov. 2014, pp. 1926-1930.

[26] M. Hussain and N. Michelusi , "Energy-efficient interactive beam alignment for millimeter-wave networks," *IEEE Trans. Wireless Commun.*, vol. 18, no. 2, pp. 838-851, Feb. 2019

[27] N. González-Prelcic, R. Méndez-Rial, and R. W. Heath, "Radar aided beam alignment in mmWave V2I communications supporting antenna diversity," in Proc. *IEEE Inf. Theory Appl. Workshop (ITA)*, Jan. 2016, pp. 1–7.

[28] I. Mavromatis, A. Tassi, R. J. Piechocki, and A. Nix, "Beam alignment for millimetre wave links with motion prediction of autonomous vehicles," in Proc. *IET Conf.*, Apr. 2017, pp. 1-8.

[29] K. Gatsis, A. Ribeiro, and G. J. Pappas, "State-based communication design for wireless control systems," in Proc. *IEEE Int. Conf. Decision Control*, Dec. 2016, pp. 129-134.

[30] Q. Li, Y. Shi, J. F. Pan, B. G. Xu, and H. X. Li, "Robust control for a networked direct drive linear motion control system: Design and experiements," *Inf. Sci.*, vol. 370-371, pp. 725-742, Nov. 2016.

[31] Q. Li, Y. Shi, J. F. Pan, B. G. Xu, and H. X. Li, "Contour tracking control of networked motion control system using improved equivalent-input-disturbance approach," *IEEE Trans. Indus. Electronics* , vol. 68, no. 6, pp. 5155-5165, May 2020.

[32] C. Wei et al., "Risk-based autonomous vehicle motion control with considering human driver's behaviour," *Transp. Res. C, Emerg. Technol.*, vol. 107, pp. 1-14, Oct. 2019.

[33] B. Chang, L. Zhang, L. Li, G. Zhao, and Z. Chen, "Optimizing resource allocation in URLLC for real-time wireless control systems," *IEEE Trans. Veh. Tech.*, vol. 68, no. 9, pp. 8916-8927, Sept. 2019.

[34] B. Chang, L. Li, G. Zhao, Z. Chen, and M. A. Imran, "Autonomous D2D transmission scheme in URLLC for real-time wireless control systems," *IEEE Trans. Commun.*, accepted, Apr. 2021.
[35] S. Cai and V. Lau, "Zero MAC latency sensor networking for cyber-physical systems," *IEEE Trans. Signal Process.*, vol. 66, no. 14, pp. 3814-3823, Jul. 2018.
[36] B. Chang, G. Zhao, L. Zhang, M. A. Imran, Z. Chen, and L. Li, "Dynamic communication QoS design for real-time wireless control systems," *IEEE Sensors J.*, vol. 20, no. 6, pp. 3005-3015, Mar. 2020.
[37] A. Boulogeorgos, E. N. Papasotiriou, and A. Alexiou, "Analytical performance assessment of THz wireless systems," *IEEE Access*, vol. 7, no. 1, pp. 1-18, Jan. 2019.
[38] A. A. Farid and S. Hranilovic, "Outage capacity optimization for freespace optical links with pointing errors," *J. Lightw. Technol.*, vol. 25, no. 7, pp. 1702-1710, Jul. 2007.
[39] P. Park, J. Araújo, and K. H. Johansson, "Wireless networked control system co-design," in Proc. *IEEE Inter. Conf. Netw., Sensing Control*, 2011, pp. 486-491.

Bo Chang received his Ph.D. from University of Electronic Science and Technology of China (UESTC) in 2020. From May 2019 to May 2020, he was a visiting student at University of Glasgow, UK. Since August 2020, he has been with the National Key Lab. on Communications, UESTC, where he is currently a Research Fellow. His research interests include ultra-reliable and low-latency communications, communication and control co-design for Industrial Internet-of-Things (IIoT), autonomous systems, and remote control of robotics in 5G/6G.

Xiaoyu Yan was born in Gansu,China, in 1996. She received her Bachelor degree from the Southwest Jiaotong University, in 2019. She is currently pursuing a Master degree in the University of Electronic Science and Technology of China. Her research interests include ultra-reliable and low-latency communications, terahertz communications, industrial internet-of-things, communication and control co-design, and cyber-physical systems.

Lei Zhang received his Ph.D. from the University of Sheffield, U.K. Dr. Lei Zhang is a Senior Lecturer at the University of Glasgow. He has academia and industry combined research experience on wireless communications and networks, and distributed systems for IoT, blockchain, autonomous systems. His 20 patents (including 17 international PCT patents) are granted/filed in 30+ countries/regions. He published 3 books, and 150+ papers in peer-reviewed journals, conferences and edited books. Dr. Zhang is an associate editor of IoT Journal, IEEE Wireless Communications Letters and Digital Communications and Networks, and a guest editor of IEEE JSAC. He received the IEEE ComSoc TAOS Technical Committee Best Paper Award 2019 and IEEE ICEICT'21 Best Paper Award. Dr. Zhang is the founding Chair of IEEE Special Interest Group on Wireless Blockchain Networks in Cognitive Networks Technical Committee (TCCN). He delivered tutorials in IEEE ICC, IEEE Globecom, IEEE VTC, IEEE PIMRC, IEEE ICBC and EUSIPCO. Dr. Zhang's research is broadly covered by media including BBC and Bloomberg.

Zhi Chen (SM'16) received B.E., M.E., and Ph.D. degrees in electrical engineering from the University of Electronic Science and Technology of China (UESTC), in 1997, 2000, and 2006, respectively. On April 2006, he joined the National Key Lab of Science and Technology on Communications (NCL), UESTC, and worked as a Professor with this lab from August 2013. He was a Visiting Scholar with the University of California, Riverside during 2010–2011. He is also the Deputy Director of Key Laboratory of Terahertz Technology, Ministry of Education. His current research interests include Terahertz communication, 5G mobile communications and tactile internet.

Lingxiang Li (S'13, M'17) received her M.S. and Ph.D. degrees in Electrical Engineering from University of Electronic Science and Technology of China (UESTC), Chengdu, China, in 2013 and 2017, respectively. She was a visiting Ph.D. student under supervisor of Prof. Athina P. Petropulu at Rutgers, The State University of New Jersey during 2015-2016. She is currently an Associate Professor with UESTC. Her research interests cover various aspects of wireless communications, networking, and signal processing, currently focusing on Terahertz communications, joint sensing and communications.

Muhammad Ali Imran (M'03, SM'12) Fellow IET, Senior Member IEEE, Senior Fellow HEA is Dean University of Glasgow UESTC and a Professor of Wireless Communication Systems with research interests in self organised networks, wireless networked control systems and the wireless sensor systems. He heads the Communications, Sensing and Imaging (CSI) research group at University of Glasgow and is Director of Centre for Educational Development and Innovation. He is an Affiliate Professor at the University of Oklahoma, USA; Adjunct Research Professor at Ajman University, UAE and a visiting Professor at 5G Innovation Centre, University of Surrey, UK. He has over 20 years of combined academic and industry experience with several leading roles in multi-million pounds funded projects. He has filed 15 patents; has authored/co-authored over 400 journal and conference publications; has authored 2 books, edited 8 books and authored more than 30 book chapters; has successfully supervised over 40 postgraduate students at Doctoral level. He has been a consultant to international projects and local companies in the area of self-organised networks.